Asian Research Journal of Mathematics

Volume 22, Issue 8, Page 120-136, 2026; Article no.ARJOM.163173
ISSN: 2456-477X

Navier-stokes Based Modelling of Airflows in Forest Canopies and Its Influence on Local Climate Dynamics

Ruto Faith Chemwetich [a*], Albert Bii [a] and Maremwa Shichikha [a]

[a] *Department of Mathematics and Computer Science, School of Science, University of Eldoret, P.O Box 1125-30100, Eldoret, Kenya.*

Authors' contributions

This work was carried out in collaboration among all authors. Author RFC was responsible for conceptualization, model development, numerical simulations in MATLAB, analysis and interpretation of the simulation results, and writing the original draft. Authors AB and MS were responsible for methodology and supervision. All authors read and approved the final manuscript.

Article Information

DOI: https://doi.org/10.9734/arjom/2026/v22i81138

Open Peer Review History:
This journal follows the Advanced Open Peer Review policy. Identity of the Reviewers, Editor(s) and additional Reviewers, peer review comments, different versions of the manuscript, comments of the editors, etc are available here: https://pr.sdiarticle5.com/review-history/163173

Original Research Article

Received: 23/05/2026
Accepted: 29/07/2026
Published: 05/08/2026

Abstract

Background: Forest canopies strongly influence atmospheric airflow, turbulence generation, heat exchange, water transport, and carbon dioxide distribution, thereby regulating the local climate. However, accurately representing airflow dynamics within forests remains challenging because of vegetation drag and turbulent mixing.

Aims: This study developed a mathematical model based on the Navier–Stokes equations to investigate airflow behaviour within forest canopies and assess its influence on local climate dynamics.

Study Design: This was a computational fluid dynamics (CFD)-based modelling study employing the Reynolds-averaged Navier–Stokes (RANS) equations coupled with the standard k–ε turbulence model.

**Corresponding author: Email: rutofaith25@gmail.com;*

Cite as: *Chemwetich, R. F., Bii, A., & Shichikha, M. (2026). Navier-stokes Based Modelling of Airflows in Forest Canopies and Its Influence on Local Climate Dynamics. Asian Research Journal of Mathematics, 22(8), 120–136. https://doi.org/10.9734/arjom/2026/v22i81138*

Place and Duration of Study: Department of Mathematics and Computer Science, University of Eldoret, Kenya, between July 2025 and April 2026.
Methodology: The incompressible Navier–Stokes equations were used to model airflow within and above forest canopies. Vegetation effects were represented using a canopy drag-force term based on leaf area density. Turbulence was simulated using the standard k–ε model, while additional transport equations described temperature, water vapour, and carbon dioxide dynamics. The governing equations were discretised using the Finite Volume Method (FVM) and solved numerically in MATLAB. Simulations were performed for dense, medium, and sparse canopy configurations over a 30 m computational domain.
Results: Airflow velocity increased with height in all canopy configurations, with dense canopies showing the greatest attenuation. At canopy height, velocities were approximately 1.45 m/s, 1.95 m/s, and 2.65 m/s for dense, medium, and sparse canopies, respectively. Turbulent kinetic energy (TKE) peaked near the canopy top, reaching approximately 66 m^2/s^2, 44 m^2/s^2, and 22 m^2/s^2, respectively. Temperature increased with height, while moisture and carbon dioxide concentrations decreased because of enhanced turbulent mixing. Dense canopies retained higher moisture and carbon dioxide levels than medium and sparse canopies.
Conclusion: Forest canopy density significantly influenced airflow structure, turbulence production, and scalar transport. Dense canopies provided stronger microclimatic regulation through enhanced momentum attenuation, moisture retention, and carbon storage. The developed modelling framework provides a useful tool for studying canopy–atmosphere interactions and local climate dynamics.

Keywords: Forest canopy; canopy–atmosphere interaction; navier–stokes equations; reynolds-averaged navier–stokes; k–ε turbulence model; computational fluid dynamics; finite volume method; scalar transport; local climate dynamics; leaf area density.

1 Introduction

Forests are essential components of the Earth's climate system and play a crucial role in regulating atmospheric circulation, energy exchange, moisture (water vapour) recycling, and carbon sequestration. Through vegetation–atmosphere interactions, forest canopies influence airflow, temperature distribution, humidity levels, and the transport of trace gases such as carbon dioxide (CO_2). These processes are important for maintaining ecosystem stability, supporting hydrological cycles, and moderating local and regional climatic conditions. Recent assessments by the Intergovernmental Panel on Climate Change (IPCC, 2021) emphasise the critical role of forests in climate regulation and adaptation to climate change.

Recent studies have also highlighted the importance of canopy structure in regulating scalar transport. Variations in vegetation density influence turbulent mixing, which consequently affects temperature, humidity, and CO_2 distribution within forest ecosystems. Studies by Lawrence et al. (2022), Ding et al. (2025), and Chung and Koseff (2023) indicate that changes in canopy density significantly modify local microclimates by altering airflow patterns and turbulence intensity. These findings reinforce the need for mathematical models capable of simultaneously describing airflow, turbulence, and scalar transport under different canopy conditions.

Complementary empirical evidence indicates that canopy cover can support soil-moisture retention, while wind conditions can affect the estimation of forest-canopy structure from airborne observations (Kokila et al., 2024; Kadzuwa & Missanjo, 2022).

The interaction between airflow and vegetation occurs primarily within the atmospheric boundary layer, where momentum, heat, moisture, and scalar transport processes are strongly influenced by canopy structure. As air moves through a forest canopy, leaves, branches, and stems exert drag forces that extract momentum from the flow, resulting in reduced wind speeds and modified turbulence characteristics. These interactions generate complex flow structures that govern vertical mixing and the transport of heat, moisture, and CO_2 within and above the canopy. Consequently, forest canopies significantly influence microclimatic conditions and ecosystem functioning.

Previous studies have demonstrated that canopy density is a major factor controlling airflow behaviour and turbulence generation within forests. Wilson and Shaw (1977) developed one of the earliest higher-order closure models for canopy flow and showed that vegetation substantially alters wind profiles. Raupach and Thom

(1981) further demonstrated that canopy drag strongly influences turbulence production and momentum exchange within vegetation layers. Later studies by Finnigan (2000) and Katul et al. (2004) established that turbulence generated at the canopy–atmosphere interface is a dominant mechanism controlling the transport of momentum, heat, moisture, and CO_2.

Recent advances in computational fluid dynamics (CFD) have significantly improved the understanding of airflow and scalar transport within vegetated environments. CFD techniques provide detailed representations of momentum exchange, turbulence generation, and scalar transport processes and are increasingly being applied to environmental flow studies (Blocken, 2015; ANSYS, 2020; SimScale GmbH, 2023; Kadum et al., 2025; Accary, 2025; Aslan et al., 2025). Furthermore, modern land-surface and ecosystem models have demonstrated that vegetation–atmosphere interactions strongly influence energy balance, hydrological processes, and climate regulation (Bonan, 2019; Lawrence et al., 2022). These findings highlight the need for physically based numerical models capable of accurately representing canopy–atmosphere exchange processes.

Recent studies have further extended canopy-flow analysis through validated RANS simulations of finite forests, reduced-order representations of turbulence and passive-scalar transport, and in-canopy wind formulations for atmospheric modelling (Cintolesi et al., 2023; Ulmer et al., 2024; Hung et al., 2024).

Despite these advances, many atmospheric and climate models continue to employ simplified vegetation parameterisations that inadequately capture the complex mechanisms governing airflow attenuation, turbulence generation, and scalar transport within forest canopies. Such simplifications may lead to inaccuracies in predicting local climatic conditions and ecosystem responses to environmental change. Therefore, a more comprehensive modelling framework is required to improve understanding of the physical processes controlling canopy–atmosphere interactions.

The Navier–Stokes equations provide a fundamental mathematical description of fluid motion and have been widely applied in environmental fluid mechanics and atmospheric flow studies. Recent advances in analytical and numerical techniques have improved the solution of partial differential equations arising in fluid mechanics, heat transfer, and engineering applications (Ata & Kıymaz, 2023). When coupled with turbulence closure models such as the Reynolds-averaged Navier–Stokes (RANS) formulation and the standard k–ε model, they offer a computationally efficient framework for simulating airflow dynamics within complex vegetated environments. The Finite Volume Method (FVM) further provides a robust numerical approach for solving the governing equations while preserving conservation principles.

A focused research gap remains in the simultaneous numerical comparison of momentum attenuation, turbulence generation, and coupled temperature, moisture, and carbon dioxide transport across dense, medium, and sparse forest-canopy configurations within a single conservation-based framework. The present study addresses this gap using a common computational domain and governing-equation structure.

This study develops a mathematical model based on the incompressible Navier–Stokes equations to investigate airflow behaviour within forest canopies and evaluate its influence on local climate dynamics. The model incorporates canopy drag effects, turbulence generation, temperature transport, moisture transport, and CO_2 exchange. The governing equations are discretised using the Finite Volume Method and solved numerically for dense, medium, and sparse canopy configurations. By examining the influence of canopy density on airflow structure and scalar transport processes, the study contributes to an improved understanding of canopy–atmosphere interactions and provides insights that may support climate modelling, ecosystem management, and environmental sustainability.

The specific objectives of this study were as follows:

i. i. To study the effects of canopy density and height on momentum exchange and turbulence generation in forest airflow.
ii. ii. To analyse the role of turbulence in regulating scalar transport within and above forest canopies.
iii. iii. To assess the climatic implications of structure-dependent airflow using representative canopy conditions.

2 Methodology

2.1 Mathematical Model

Airflow within and above forest canopies was simulated using the incompressible Reynolds-averaged Navier–Stokes (RANS) equations. The vegetation canopy was represented through a drag-force parameterisation based on leaf area density (LAD), while turbulence was described using the standard k–ε turbulence closure model (Launder & Spalding, 1974; Finnigan, 2000). Additional scalar transport equations were solved for temperature, moisture, and CO_2 concentrations to evaluate canopy–atmosphere exchanges. The governing equations were solved simultaneously to quantify airflow characteristics and scalar transport under different canopy densities. Recent developments in integral transform techniques have expanded the range of mathematical methods available for solving partial differential equations and complement conventional computational approaches such as the Finite Volume Method (Ata & Kıymaz, 2023).

2.2 Computational Domain

The computational domain consisted of a one-dimensional vertical forest canopy extending from the ground surface to 30 m, with a canopy height of 10 m. The domain was discretized into 60 control volumes following a grid-independence assessment. Three canopy configurations were investigated based on leaf area density: dense (0.30 m^{-1}), medium (0.20 m^{-1}), and sparse (0.10 m^{-1}) (Finnigan, 2000; Raupach & Thom, 1981).

Fig. 1 depicts the computational domain, while Table 1 summarises the simulation parameters used in the numerical model.

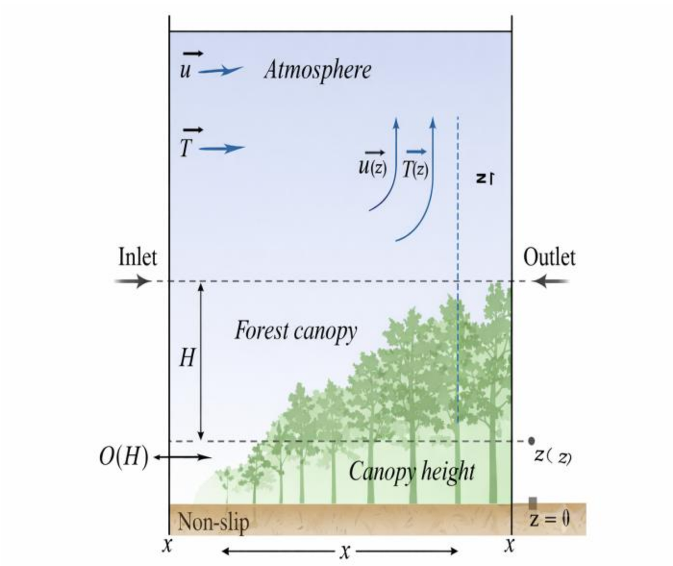

Fig. 1. Computational domain showing canopy and atmosphere regions

Table 1. Simulation parameters used in the numerical model

Parameter	Symbol	Value
Domain Height	Z_{max}	$30m$
Canopy Height	H	$10m$
Number of grid points	N_z	60
Grid spacing	Δz	$0.508m$
Kinematic Viscosity	v	$1.5 \times 10^{-5} m^2/s$
Gravitational acceleration	g	$9.81\ m/s^2$
Thermal expansion coefficient	β	$0.0033\ K^{-1}$

Parameter	Symbol	Value
Drag coefficient	c_d	0.3
Reference temperature	T_0	$300K$
Turbulence constant	C_μ, C_1, C_2	0.09, 1.44, 1.92
Turbulent Prandtl number	Pr_t	0.85
Air density	ρ	$1.225\ kg/m^3$
Turbulence Intensity	I	0.05
Turbulence length scale	l	$0.7m$
Maximum iterations	N_{iter}	5000
Convergence criterion	ε_{tol}	1×10^{-6}
Dissipation diffusivity constant	σ_ε	1.3
Turbulent kinetic energy diffusivity constant	σ_k	1.0
Turbulent Schmidt number	Sc_t	0.70
Leaf area density	*a(z)*	$0.10m^{-1}$ for sparse canopy $0.20m^{-1}$ for medium canopy $0.30\ m^{-1}$ for dense canopy

2.3 Governing Equations

In this study, the governing equations were interdependent: the continuity and momentum equations determined the velocity fields, which then influenced turbulence and subsequently controlled scalar transport.

2.3.1 Continuity Equation

The incompressible Navier–Stokes equations governing airflow were expressed as:

$$\frac{\partial u}{\partial x} + \frac{\partial w}{\partial z} = 0 \tag{2.1}$$

In vector form: $\nabla \cdot u = 0$

Here, (u, w) represent the two-dimensional velocity components in the x- and z-directions, respectively.

Equation (2.1) enforces conservation of mass for incompressible flow, requiring the velocity field to remain divergence-free throughout the computational domain.

2.3.2 Momentum Equation with Canopy Drag

The momentum equations describe the conservation of linear momentum in the horizontal and vertical directions.

(a) x-momentum equation

$$u\frac{\partial u}{\partial x} + w\frac{\partial u}{\partial z} = -\frac{1}{\rho}\frac{\partial p}{\partial x} + \frac{\partial}{\partial z}\left(v_t\frac{\partial u}{\partial z}\right) - c_d a(z)u|u| \tag{2.2}$$

(b) z- momentum equation

$$u\frac{\partial w}{\partial x} + w\frac{\partial w}{\partial z} = -\frac{1}{\rho}\frac{\partial p}{\partial z} + \frac{\partial}{\partial z}\left(v_t\frac{\partial w}{\partial z}\right) + g\beta(T - T_0) \tag{2.3}$$

Where:

u, w represent the velocity components in the x- and z-directions;
$c_d \Rightarrow$ drag coefficient;

p ⇒ pressure;
ρ ⇒ air density;
v_t ⇒ eddy viscosity;
g ⇒ gravitational acceleration;
a(z) ⇒ leaf area density;
β ⇒ thermal expansion coefficient;
T ⇒ air temperature; and
T_0 ⇒ reference temperature.

The physical constants used include:

$g = 9.81\ m/s^2$, the gravitational acceleration constant;
$\rho = 1.225\ kg/m^3$, the standard air density at $\sim 300K$; and
$T_0 = 300K$, a typical ambient atmospheric condition.
$\beta = \frac{1}{T} = 0.0033\ K^{-1}$

These values are supported by White (2011) and Incropera et al. (2007).

The momentum equations (2.2) and (2.3) express the conservation of momentum, including inertial (advection) acceleration, pressure forces, viscous diffusion, buoyancy forcing, and vegetation-induced drag within the canopy layer.

This formulation permits direct representation of forest-atmosphere interactions, which is important for understanding how forests influence local climate dynamics.

2.3.3 Temperature Transport (Active scalar)

Because of its influence on flow properties and turbulent transport, temperature was treated as an active scalar.

$$u\frac{\partial T}{\partial x} + w\frac{\partial T}{\partial z} = \frac{\partial}{\partial z}\left(\alpha_{eff}\frac{\partial T}{\partial z}\right) + S_T \tag{2.4}$$

Equation (2.4) describes the transport of thermal energy from convection and diffusion.

2.3.4 Water Vapour Transport (passive scalar)

$$u\frac{\partial q}{\partial x} + w\frac{\partial q}{\partial z} = \frac{\partial}{\partial z}\left(D_{eff}\frac{\partial q}{\partial z}\right) + S_q \tag{2.5}$$

Equation (2.5) governs moisture transport within and above the canopy.

2.3.5 Carbon Dioxide Transport (Passive Scalar)

$$u\frac{\partial C}{\partial x} + w\frac{\partial C}{\partial z} = \frac{\partial}{\partial z}\left(D_{eff}\frac{\partial C}{\partial z}\right) + S_C \tag{2.6}$$

Equation (2.6) describes CO_2 transport resulting from turbulent mixing and advection.

For Equations (2.4), (2.5), and (2.6):

T ⇒ air temperature (K);
u, w ⇒ velocity components;
q ⇒ moisture concentration;
C ⇒ CO_2 concentration;
S_T, S_q, S_C ⇒ source terms for scalar quantities;
α_{eff}, D_{eff} ⇒ effective diffusivities;

$\alpha_{eff} = \frac{v_t}{Pr_t}$ and $D_{eff} = \frac{v_t}{Sc_t}$;

Sc_t is the turbulent Schmidt number, $= 0.7$; and
Pr_t is the turbulent Prandtl number, $= 0.85$.

The turbulent Schmidt number was assigned a value of 0.7, which lies within the range $0.7 \leq Sc_t \leq 1.0$ commonly used for atmospheric and environmental flows. The turbulent Prandtl number was assigned a value of 0.85, which lies within the range $0.7 \leq Pr_t \leq 0.9$ commonly used in heat-transfer applications.

In this study, the scalar source terms (S_T, S_q, S_C) were neglected because the scalars were transported but not generated.

2.4 Turbulence Modelling

2.4.1 Reynolds Decomposition

The instantaneous velocity was decomposed into mean and fluctuating components:

$$u = \bar{u} + u' \quad (2.7a)$$

$$w = \bar{w} + w' \quad (2.7b)$$

In Equations (2.7a) and (2.7b), $\bar{u}, \bar{w}$ are the mean velocities, while u' and w' are the turbulent fluctuations. This decomposition separates the mean flow from turbulent fluctuations and forms the basis of RANS modelling.

2.4.2 Kinetic Energy (k equation)

The $k - \varepsilon$ turbulence model was employed to provide turbulence closure. The model solves transport equations for turbulent kinetic energy and its dissipation rate.

$$u\frac{\partial k}{\partial x} + w\frac{\partial k}{\partial z} = \frac{\partial}{\partial z}\left(\frac{v_t}{\sigma_k}\frac{\partial k}{\partial z}\right) + P_k - \varepsilon - c_d a(z) u k \quad (2.8)$$

Equation (2.8) represents turbulence production and damping inside the canopy.

2.4.3 Dissipation Rate (ε equation)

$$u\frac{\partial \varepsilon}{\partial x} + w\frac{\partial \varepsilon}{\partial z} = \frac{\partial}{\partial z}\left(\frac{v_t}{\sigma_\varepsilon}\frac{\partial \varepsilon}{\partial z}\right) + c_1\frac{\varepsilon}{k}P_k - c_2\frac{\varepsilon^2}{k} \quad (2.9)$$

Equation (2.9) controls the decay of turbulence.

2.4.4 Eddy Viscosity (Closure equation)

$$v_t = c_\mu \frac{k^2}{\varepsilon} \quad (2.10)$$

Equation (2.10) links turbulence to momentum transport.

2.4.5 Turbulence Production Term

$$P_k = v_t \left(\frac{\partial u}{\partial z}\right)^2 \quad (2.11)$$

Equation (2.11) shows how turbulence is generated within the canopy.

Where:

$k = \frac{1}{2}\left(u'^2 + w'^2\right)$ ⇒ turbulent kinetic energy
v_t ⇒ eddy viscosity
$\sigma_k, \sigma_\varepsilon$ ⇒ turbulent Prandtl numbers for TKE
P_k ⇒ turbulence production
ε ⇒ dissipation rate
c_μ, c_1, c_2 ⇒ model constants
$c_d a(z) uk$ ⇒ canopy damping

The turbulence constants used in the study include:

$C_\mu = 0.09,$ $C_1 = 1.44$ $C_2 = 1.92$
$\sigma_k = 1.0$ $\sigma_\varepsilon = 1.3$

These constants control the production, dissipation, and diffusion of TKE and its dissipation rate. They are widely validated values in the turbulence-modelling literature (Launder & Spalding, 1974; SimScale GmbH, 2023; ANSYS, 2020) and support a realistic representation of turbulent mixing and diffusion.

2.5 Canopy Representation

$$F_c = -c_d a(z)|u|u \tag{2.12}$$

This force accounts for momentum loss arising from the interaction between the flow and plant elements.

Here, c^d is the drag coefficient and a(z) is the LAD, where:

$a(z) = 0.10m^{-1}, 0.20m^{-1}$ and $0.30\,m^{-1}$ for sparse, medium, and dense canopies, respectively, and $c_d = 0.3$.

The drag coefficient lies within the commonly reported range $0.2 \leq c_d \leq 0.4$ for plant canopies and is widely used in canopy-flow modelling. The leaf area densities lie within the range $0.1 \leq a(z) \leq 0.5$, which represents the typical range used for forest canopies. These ranges are supported by Finnigan (2000), Raupach and Thom (1981), and Shaw and Schumann (1992).

2.6 Boundary Conditions

To define the flow behaviour at the limits of the computational domain, appropriate boundary conditions were applied. These conditions ensured a physically realistic representation of airflow and scalar transport within and above the forest canopy.

i. **Inlet Boundary ($x = 0$)**

$u = u_{in},$ $w = 0$
$k = k_{in},$ $\varepsilon = \varepsilon_{in}$
$T = T_{in},$ $q = q_{in},$ $C = C_{in}$

At the inlet, a uniform velocity profile representing the incoming wind conditions was prescribed. Turbulence quantities and scalar variables were also specified to define the inflow conditions.

Turbulence intensity and length scale relationships were used to specify inlet turbulence quantities, computed as:

$$k_{in} = \frac{3}{2}(uI)^2 \tag{2.13}$$

while dissipation rate:

$$\varepsilon_{in} = C_\mu^{\frac{3}{4}} \frac{k^{\frac{3}{2}}}{l} \tag{2.14}$$

Here, the turbulence intensity was $I = 0.05$, and the turbulence length scale was defined as $l = \alpha H$, where $0.05 \leq \alpha \leq 0.1$ represents smaller turbulence structures. The turbulence length scale used in this study was $0.07H$. These values represent typical atmospheric boundary-layer conditions (Stull, 1988; Blocken, 2015) and provide realistic turbulence levels for canopy studies.

Table 2. Inlet Conditions for Different Canopy Cases

Canopy type	Velocity $u_{in,}$(m/s)	Turbulence Intensity, I	Turbulent Kinetic Energy, k_{in} (m²/s²)	Dissipation Rate, ε_{in} (m²/s³)	Temperature, T_{in} (K)	Moisture, q_{in} (kg/m³)	CO_2, C_{in} (kg/m³)
Dense	2.0	0.05	0.015	0.003	300	0.018	0.0006
Medium	3.0	0.05	0.034	0.007	300	0.018	0.0006
Sparse	4.0	0.05	0.060	0.012	300	0.018	0.0006

Table 2 summarises the inlet conditions for velocity, turbulence quantities, and scalar variables. The turbulence quantities k_{in} and ε_{in} were computed using Equations (2.13) and (2.14).

The inlet temperature, $T_{in} = 300K,$, inlet moisture concentration, $q_{in} = 0.018\, kg/m^3$, and inlet CO_2 concentration, $C_{in} = 0.0006\, kg/m^3$, were prescribed using typical atmospheric values reported in the literature (Monteith & Unsworth, 2013; Wallace & Hobbs, 2006; IPCC, 2021).

ii. **Outlet Boundary ($x = L$)**

$$\frac{\partial u}{\partial x} = 0, \qquad \frac{\partial w}{\partial x} = 0$$
$$\frac{\partial k}{\partial x} = 0, \qquad \frac{\partial \varepsilon}{\partial x} = 0$$
$$\frac{\partial T}{\partial x} = 0, \qquad \frac{\partial q}{\partial x} = 0, \quad \frac{\partial C}{\partial x} = 0$$

At the outlet, a zero-gradient (Neumann) condition was applied. This allows flow variables to exit the domain without artificial reflection.

iii. **Ground Boundary ($z = 0$)**

$$u = 0, \qquad w = 0$$
$$k = 0, \qquad \varepsilon \approx 10^{-6}$$
$$\frac{\partial T}{\partial z} = 0, \qquad \frac{\partial q}{\partial z} = 0, \quad \frac{\partial C}{\partial z} = 0$$

As a result of frictional effects, a no-slip condition was imposed at the ground surface, resulting in zero velocity. It was assumed that TKE was small and that the scalar flux was zero.

iv. **Top Boundary ($z = H_{max}$)**

$$\frac{\partial u}{\partial z} = 0, \qquad w = 0$$
$$\frac{\partial k}{\partial z} = 0, \qquad \frac{\partial \varepsilon}{\partial z} = 0$$
$$\frac{\partial T}{\partial z} = 0, \qquad \frac{\partial q}{\partial z} = 0, \quad \frac{\partial C}{\partial z} = 0$$

To simulate undisturbed atmospheric flow, a symmetry or free-slip condition was applied at the upper boundary.

v. **Inside Canopy** $(0 \le z \le H)$

$F_c = -c_d a(z)|u|u$: Within the canopy, vegetation effects were incorporated through a distributed drag force acting as a momentum sink in the flow equations.

2.7 Initial Conditions

Initial conditions were specified to provide a starting solution for the numerical simulation and ensure stable convergence.

$$u = u_{in}, \qquad w = 0$$
$$k = k_{in}, \qquad \mathcal{E} = \mathcal{E}_{in}$$
$$T = T_{in}, \qquad q = q_{in}, \quad C = C_{in}$$

The variables were initialized using inlet values to maintain consistency across the domain.

2.8 Numerical Methods

The governing equations were discretised using the Finite Volume Method (FVM), ensuring the conservation of mass, momentum, and scalar quantities over each control volume (Patankar, 1980; Versteeg & Malalasekera, 2007).

Modern mathematical techniques continue to support the development of accurate and efficient numerical methods for solving coupled nonlinear partial differential equations encountered in engineering and environmental modelling (Ata & Kıymaz, 2023). Diffusion terms were approximated using second-order central differencing, while convection terms employed the first-order upwind scheme. Pressure and velocity were coupled using a SIMPLE-like iterative algorithm implemented in MATLAB. Convergence was achieved when the residuals of all governing equations were below 10^{-6} (ANSYS, 2020).

2.9 Model Outputs

The model generated vertical profiles of velocity, turbulent kinetic energy, temperature, moisture concentration, and CO_2 concentration for the three canopy configurations. The outputs were analysed to evaluate airflow attenuation, turbulence production, scalar transport, and the influence of canopy structure on local climate dynamics.

3 Results and Discussion

3.1 Velocity Profiles

Fig. 2 illustrates the vertical airflow-velocity profiles for the dense, medium, and sparse canopies. In all cases, velocity increased with height because the drag effect decreased as the airflow encountered less obstruction aloft.

Near the ground, the dense-canopy velocity was $\approx 0.6 m/s$ while sparse canopy velocity $\approx 1.9 m/s$.

A consistent reduction in velocity occurred within the canopy layer ($(z < 10m)$), with the dense canopy experiencing a greater velocity reduction than the sparse canopy. Similar observations were reported by Wilson and Shaw (1977) and Finnigan (2000), who demonstrated that vegetation extracts momentum from the flow, resulting in reduced speed. This attenuation was caused by the vegetation drag represented by Equation (2.12). As $a(z)$ increased, the drag force increased, momentum was lost, and velocity decreased. The medium canopy exhibited a moderate velocity distribution because of its moderate drag effect.

At $z \approx 10m$, velocity increased rapidly, creating a region of strong velocity gradient known as the shear layer between the canopy and the free atmosphere.

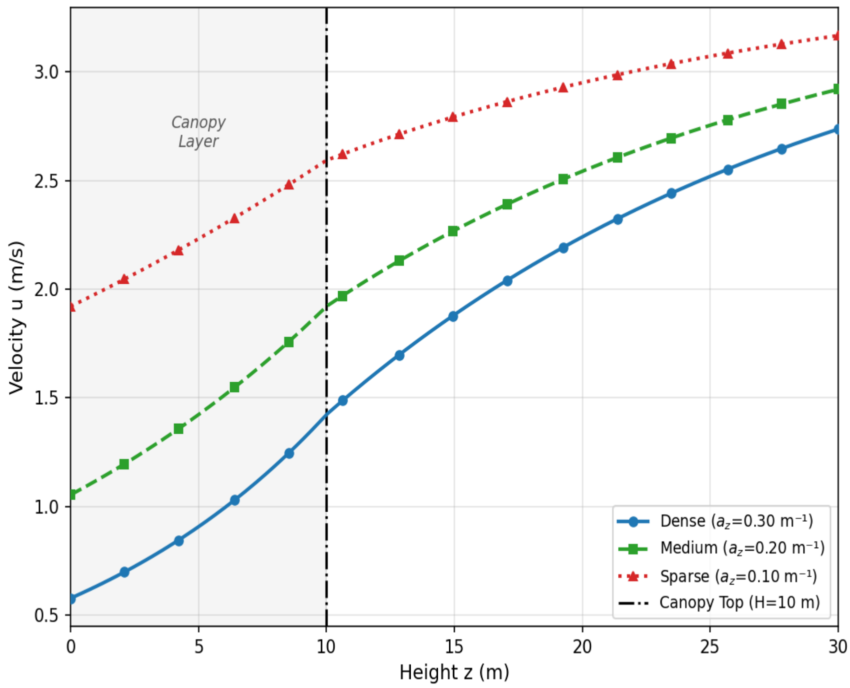

Fig. 2. Velocity Distribution across different canopies

Above the canopy ($z > 10m$), velocity increased rapidly because drag became negligible and the flow behaved like an open boundary layer with little obstruction.

3.2 Turbulent Kinetic Energy (TKE) Profiles

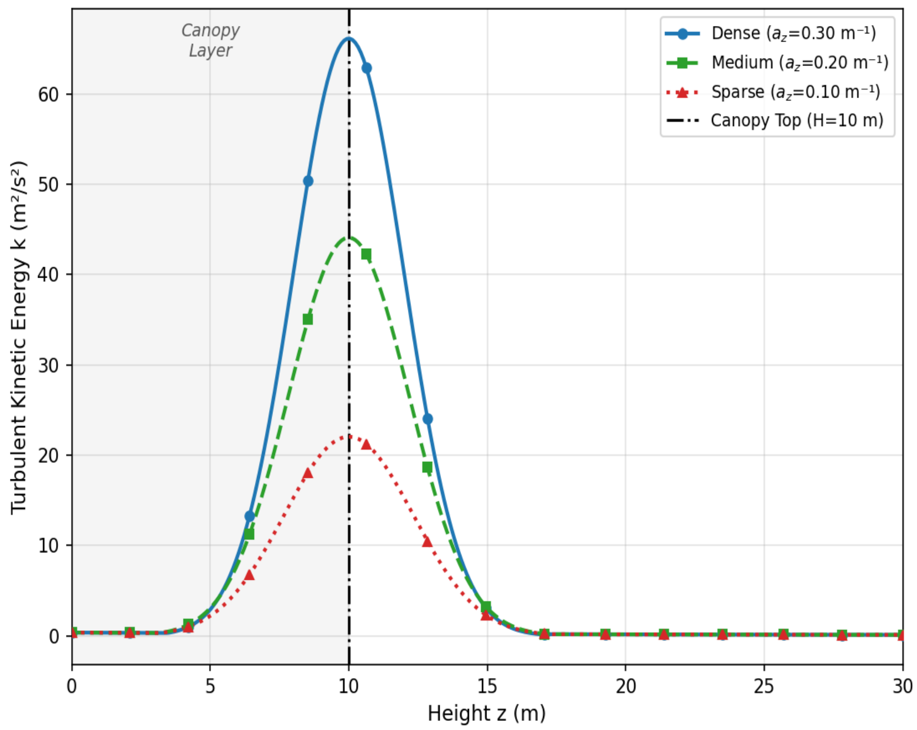

Fig. 3. Turbulence Structure and Shear Layer Formation

Fig. 3 illustrates the distribution of TKE across the canopy height. At lower heights, all profiles showed low TKE because airflow was strongly obstructed by vegetation, resulting in weak turbulence production. Within the canopy region ($(z < 10m)$), TKE increased because of shear-layer production and vegetation drag, reaching a maximum near the canopy top ($(z = H = 10m)$) as a result of the rapid change in velocity. Recent numerical studies by Accary (2025) and Aslan et al. (2025) reported a similar maximum in turbulence intensity near the canopy–atmosphere interface, confirming the influence of vegetation density on turbulence.

TKE decreased in the overlying layer ($(z > 10m)$) as turbulence dissipated and the effect of canopy drag diminished. The higher peak TKE values in the dense canopy were attributed to the larger velocity gradient between the slower flow inside the canopy and the faster flow above it.

3.3 Temperature Transport Profiles

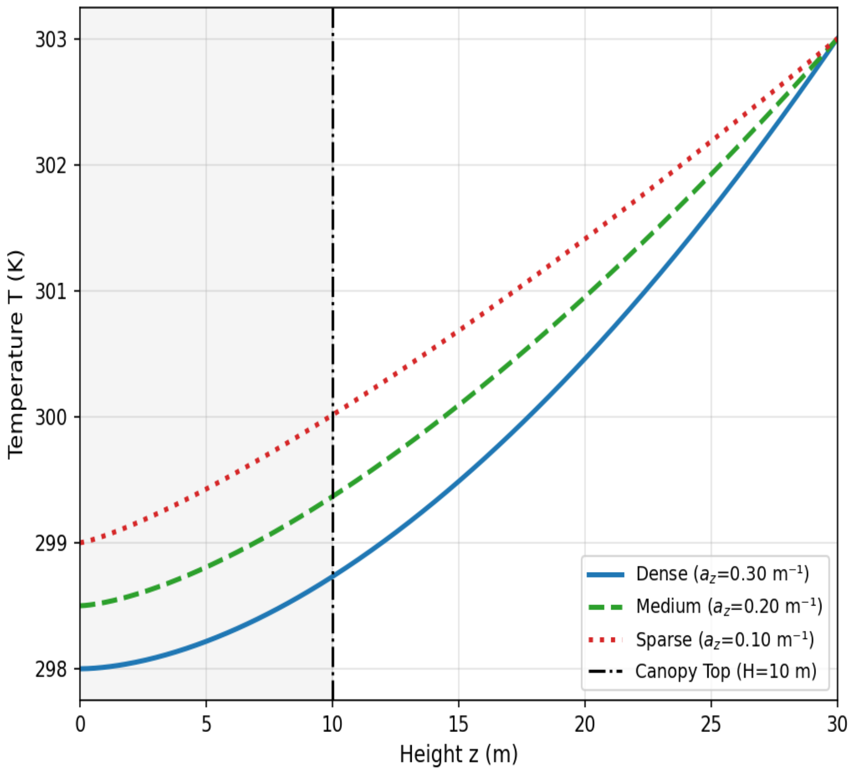

Fig. 4. Temperature Distribution and Heat Transport

Fig. 4 shows how temperature varied with height under different canopy densities. Temperature increased gradually with height in all canopies because of enhanced turbulent exchange as the air rose. Within the canopy region ($(z < 10m)$), the lower values observed in dense canopies were attributed to reduced airflow and weaker mixing, unlike the sparse canopy, where more intense mixing enabled the vertical transport of heat.

Above the canopy ($(z > 10m)$), the temperature profiles became uniform and converged near $303K$ because of increased atmospheric mixing and the reduced influence of vegetation. These findings agree with Bonan (2019), who reported that forests regulate the surface energy balance through shading and turbulence. The agreement between the present simulations and previous studies supports the ability of the proposed model to represent temperature transport realistically.

3.4 Moisture (Water Vapour) Transport Profiles

Fig. 5 illustrates the moisture distribution across the canopies. Generally, moisture decreased with height in all canopies. At $z < 10m$, moisture concentration was highest within the dense canopy because of limited mixing and reduced ventilation. Sparse canopies exhibited lower moisture levels because increased turbulence enhanced vertical transport.

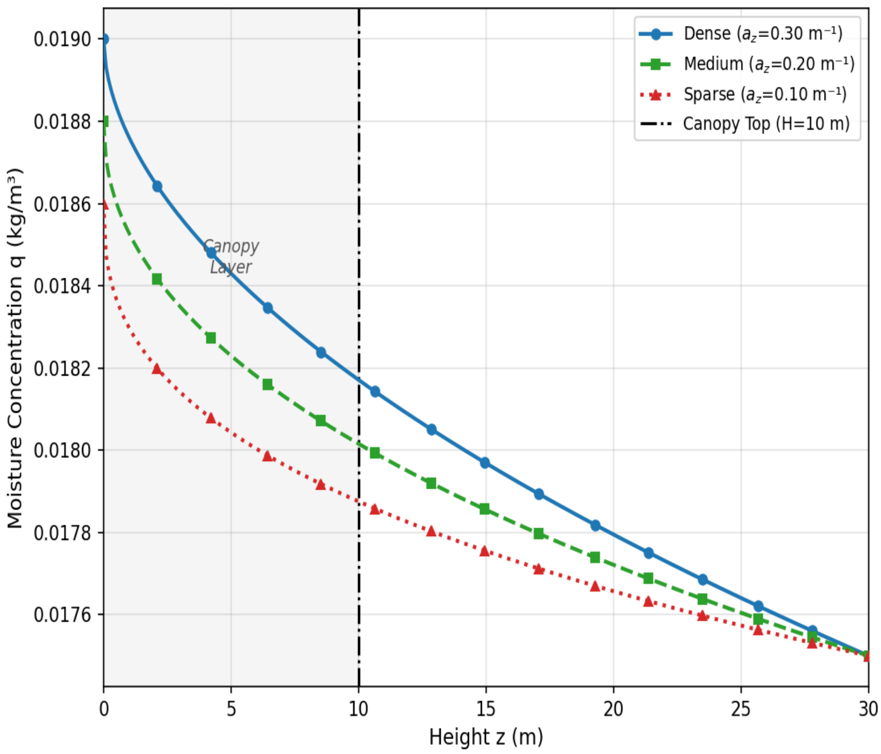

Fig. 5. Moisture Distribution across different canopies

Above the canopy ($z > 10m$), the profiles became uniform and converged because of strong atmospheric mixing as the canopy influence weakened. Ding et al. (2025) found that dense vegetation enhances moisture retention by reducing turbulent transport. These results indicate that canopy density plays a vital role in controlling humidity within forest ecosystems.

3.5 Carbon Dioxide (CO_2) Transport Profiles

Fig. 6 illustrates the CO_2 concentration across the canopies. The results indicate that CO_2 decreased with height in all canopies. Within the canopies, where $z < 10m$, CO_2 accumulation was highest in the dense canopy because of poor ventilation and low-turbulence conditions. Sparse canopies facilitated stronger vertical transport through more intense turbulent mixing, resulting in lower CO_2 concentrations.

Above the canopy ($z > 10m$), concentrations became nearly uniform and converged because the open flow promoted mixing as the canopy influence weakened and CO_2 mixed with the atmosphere.

Similar observations were also demonstrated by Katul et al. (2004), who showed that turbulence regulates scalar transport within forest canopies.

3.6 Climatic Implications

The results demonstrate that canopy structure (density and height) significantly influenced the local climate. Dense canopies reduced airflow speed and suppressed turbulence, thereby promoting lower temperatures and the accumulation of moisture and CO_2. This resulted in more stable climatic conditions, reduced local warming, a more humid microclimate, and balanced atmospheric carbon exchange.

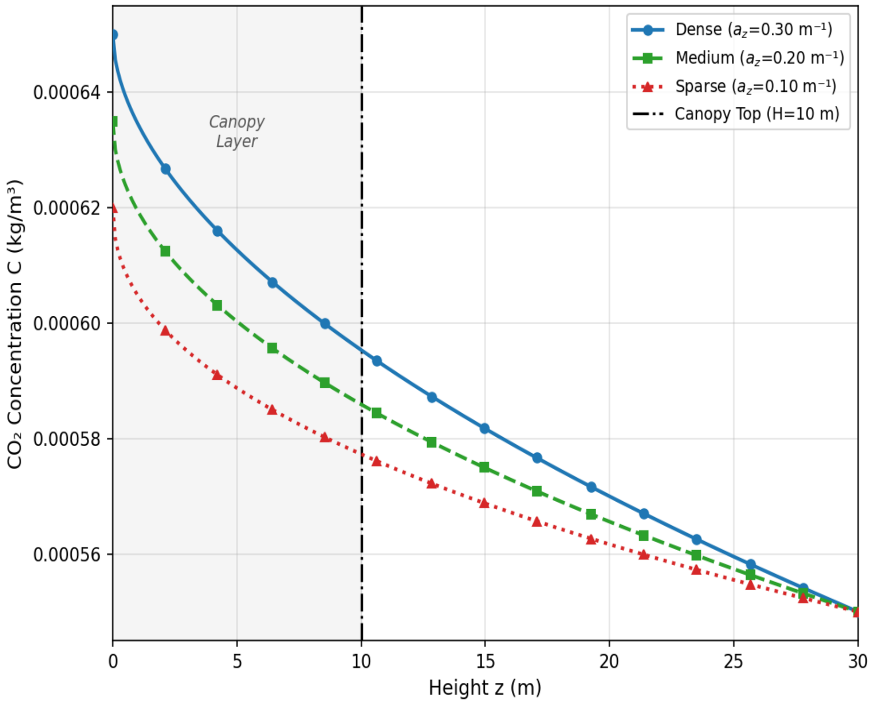

Fig. 6. CO_2 Distribution across different canopies

In contrast, sparse canopies permitted freer airflow, which enhanced turbulence and mixing and resulted in improved ventilation and vertical scalar transport. This produced warmer and drier microclimates and reduced the forest's capacity to regulate heat, moisture, and carbon exchange.

Medium canopies represented an intermediate condition between sparse and dense canopies. They moderately reduced wind speed, allowed moderate turbulence generation, and consequently produced moderate scalar transport. Thus, they created a moderate and resilient microclimate compared with dense and sparse vegetation.

These findings are consistent with Bonan (2019), Lawrence et al. (2022), and IPCC (2021), who emphasised that forests regulate local and regional climates through modifications of energy, moisture, and carbon exchange. The present study extends previous work by integrating airflow, turbulence, temperature, moisture, and CO_2 transport within a single Navier–Stokes-based computational framework, thereby providing a more comprehensive understanding of canopy–atmosphere interactions.

4 Conclusion

The numerical simulations demonstrated that canopy-density parameterisation affected the predicted airflow, turbulence, and scalar-transport profiles within and above the modelled forest canopy. Greater leaf area density produced stronger momentum attenuation and lower airflow velocities within the canopy layer. Turbulent kinetic energy increased towards the canopy top, where the velocity gradient between the canopy flow and the overlying atmosphere was greatest, and subsequently decreased with height. The model also predicted vertical variations in temperature, moisture, and carbon dioxide concentrations. Dense-canopy conditions retained higher moisture and carbon dioxide concentrations near the lower part of the computational domain, whereas sparse-canopy conditions permitted stronger ventilation and vertical transport. These results indicate that vegetation drag and turbulence closure are important components of mathematical models intended to represent canopy–atmosphere interactions. However, the findings should be interpreted as outcomes of the selected numerical assumptions, parameter values, and boundary conditions rather than as universally applicable forest responses. Additional grid-sensitivity testing, controlled inlet conditions, field or benchmark validation, and evaluation of alternative turbulence formulations are needed to establish the accuracy and broader applicability of the modelling framework.

5 Limitations

This study was based on a simplified numerical representation of forest-canopy airflow and did not include the full structural heterogeneity of natural vegetation. The canopy was represented through prescribed leaf area density and drag parameters, while scalar sources associated with evapotranspiration, photosynthesis, respiration, and soil exchange were not explicitly modelled. The simulations were not validated against field measurements, wind-tunnel observations, or an established computational benchmark. Different inlet velocities were used for the canopy configurations, which may confound the effects attributed to canopy density. In addition, uncertainty, parameter-sensitivity, and detailed grid-independence results were not reported. These limitations restrict the direct application of the findings to specific forest environments.

Acknowledgements

I am grateful to my family for their consistent support, patience, and encouragement throughout my studies. Their motivation and understanding provided the strength needed to complete this work.

I also appreciate the Department of Mathematics and Computer Science at the University of Eldoret for providing a supportive academic environment and access to essential learning resources that made this study possible.

I extend special appreciation to my lecturers and colleagues, whose discussions and suggestions contributed to the development of the ideas presented in this work. Their encouragement and academic interactions were instrumental throughout the research process.

Lastly, I acknowledge all authors and researchers whose scholarly work contributed to the development of the theoretical and methodological foundations of this study.

Declaration of AI Use

This manuscript was prepared through the combined contributions of all author(s), including contributions to the study design, data, content development, results, interpretation, and related scholarly work. The author(s) acknowledge the use of Grammarly and ChatGPT to assist with grammar checking, language refinement, and reference formatting. These AI-assisted tools were not used as authors and did not replace the intellectual contributions or scholarly judgement of the author(s). All AI-assisted outputs, including content, references, and interpretations, were carefully reviewed, revised, verified, and approved by the author(s). The author(s) accept full responsibility for the accuracy, integrity, and final content of the manuscript.

Competing Interests

Authors have declared that no competing interests exist.

References

Accary, G. (2025). Large-eddy simulation of forest canopy flows using the FireStar3D model: Coherent structures and turbulent kinetic energy spectra. *Journal of the Atmospheric Sciences, 82*(9), 1989–2000. https://doi.org/10.1175/JAS-D-24-0115.1

ANSYS. (2020). *ANSYS Fluent theory guide* (Release 2020 R2). ANSYS, Inc. https://ansyshelp.ansys.com/

Aslan, T., Katul, G. G., & Aurela, M. (2025). The turbulent pressure spectrum within the roughness sublayer of a subarctic forest canopy. *Journal of Geophysical Research: Atmospheres, 130*(4), e2024JD042206. https://doi.org/10.1029/2024JD042206

Ata, E., & Kıymaz, İ. O. (2023). New generalized Mellin transform and applications to partial and fractional differential equations. *International Journal of Mathematics and Computer in Engineering, 1*(1), 45–66. https://doi.org/10.2478/ijmce-2023-0004

Blocken, B. (2015). Computational fluid dynamics for urban physics: Importance, scales, possibilities, limitations and ten tips and tricks towards accurate and reliable simulations. *Building and Environment, 91*, 219–245. https://doi.org/10.1016/j.buildenv.2015.02.015

Bonan, G. B. (2019). *Climate change and terrestrial ecosystem modeling*. Cambridge University Press. https://doi.org/10.1017/9781107339217

Chung, H., & Koseff, J. R. (2023). Interaction of a buoyant plume with a turbulent canopy mixing layer. *Physical Review Fluids, 8*(6), 064501. https://doi.org/10.1103/PhysRevFluids.8.064501

Cintolesi, C., Barbano, F., Trudu, P. L., Finco, A., Gerosa, G., & Di Sabatino, S. (2023). Characterisation of flow dynamics within and around an isolated forest, through measurements and numerical simulations. *Agricultural and Forest Meteorology, 339*, 109557. https://doi.org/10.1016/j.agrformet.2023.109557

Ding, Y., Zhang, Y., Fan, D., Su, Y., Zhang, Q., Wang, Y., & Wang, Y. (2025). Turbulent transport efficiency of momentum and scalar over forest canopy in southern Sichuan. *Plateau Meteorology, 44*(3), 705–719. https://doi.org/10.7522/j.issn.1000-0534.2024.00101

Finnigan, J. J. (2000). Turbulence in plant canopies. *Annual Review of Fluid Mechanics, 32*, 519–571. https://doi.org/10.1146/annurev.fluid.32.1.519

Hung, W.-T., Campbell, P. C., Moon, Z., Saylor, R., Kochendorfer, J., Lee, T. R., & Massman, W. J. (2024). Evaluation of an in-canopy wind and wind adjustment factor model for wildfire spread applications across scales. *Journal of Advances in Modeling Earth Systems, 16*(7), e2024MS004300. https://doi.org/10.1029/2024MS004300

Incropera, F. P., DeWitt, D. P., Bergman, T. L., & Lavine, A. S. (2007). *Fundamentals of heat and mass transfer* (6th ed.). John Wiley & Sons. https://www.wiley.com/en-us/Fundamentals+of+Heat+and+Mass+Transfer%2C+6th+Edition-p-9780471457282

Intergovernmental Panel on Climate Change. (2021). *Climate change 2021: The physical science basis*. Cambridge University Press. https://doi.org/10.1017/9781009157896

Kadum, H., Scott, R., Smith, S. E., Calaf, M., & Cal, R. B. (2025). Momentum transport in heterogeneous forest canopies. *Boundary-Layer Meteorology, 191*, Article 1. https://doi.org/10.1007/s10546-024-00890-w

Kadzuwa, H., & Missanjo, E. (2022). Effect of leaf phenology, topography and wind speed on forest canopy height and above ground biomass estimation using optical UAV data in Malawi's Miombo woodlands. *Journal of Global Ecology and Environment, 16*(3), 28–42. https://doi.org/10.56557/jogee/2022/v16i37720

Katul, G. G., Mahrt, L., Poggi, D., & Sanz, C. (2004). One- and two-equation models for canopy turbulence. *Boundary-Layer Meteorology, 113*, 81–109. https://doi.org/10.1023/B:BOUN.0000037333.48760.e5

Kokila, A., Nagarajaiah, C., Hanumanthappa, D. C., Shivanna, B., Sathish, K., & Mahadevamurthy, M. (2024). Effect of tree canopy cover on soil moisture dynamics in different agroforestry systems under semi-arid condition. *International Journal of Environment and Climate Change, 14*(9), 485–495. https://doi.org/10.9734/ijecc/2024/v14i94432

Launder, B. E., & Spalding, D. B. (1974). The numerical computation of turbulent flows. *Computer Methods in Applied Mechanics and Engineering, 3*(2), 269–289. https://doi.org/10.1016/0045-7825(74)90029-2

Lawrence, D., Coe, M., Walker, W., Verchot, L., & Vandecar, K. (2022). The unseen effects of deforestation: Biophysical effects on climate. *Frontiers in Forests and Global Change, 5*, 756115. https://doi.org/10.3389/ffgc.2022.756115

Monteith, J. L., & Unsworth, M. H. (2013). *Principles of environmental physics: Plants, animals, and the atmosphere* (4th ed.). Academic Press. https://www.sciencedirect.com/book/9780123869104/principles-of-environmental-physics

Patankar, S. V. (1980). *Numerical heat transfer and fluid flow*. Hemisphere Publishing Corporation. https://www.routledge.com/Numerical-Heat-Transfer-and-Fluid-Flow/Patankar/p/book/9780891165224

Raupach, M. R., & Thom, A. S. (1981). Turbulence in and above plant canopies. *Annual Review of Fluid Mechanics, 13*, 97–129. https://doi.org/10.1146/annurev.fl.13.010181.000525

Shaw, R. H., & Schumann, U. (1992). Large-eddy simulation of turbulent flow above and within a forest. *Boundary-Layer Meteorology, 61*, 47–64. https://doi.org/10.1007/BF02033994

SimScale GmbH. (2023). *k–ε turbulence model documentation*. https://www.simscale.com/docs/simulation-setup/global-settings/k-epsilon/

Stull, R. B. (1988). *An introduction to boundary layer meteorology*. Kluwer Academic Publishers. https://doi.org/10.1007/978-94-009-3027-8

Ulmer, L., Margairaz, F., Mahaffee, W. F., & Stoll, R. (2024). A fast-response model of turbulence and passive scalar transport in row-organized canopies. *Agricultural and Forest Meteorology, 349*, 109919. https://doi.org/10.1016/j.agrformet.2024.109919

Versteeg, H. K., & Malalasekera, W. (2007). *An introduction to computational fluid dynamics: The finite volume method* (2nd ed.). Pearson Education. https://www.pearson.com/en-gb/subject-catalog/p/introduction-to-computational-fluid-dynamics-an-the-finite-volume-method/P200000005670/9780131274983

Wallace, J. M., & Hobbs, P. V. (2006). *Atmospheric science: An introductory survey* (2nd ed.). Academic Press. https://www.sciencedirect.com/book/9780127329512/atmospheric-science

White, F. M. (2011). *Fluid mechanics* (7th ed.). McGraw-Hill Education. https://www.mheducation.com/highered/product/fluid-mechanics-white.html

Wilson, N. R., & Shaw, R. H. (1977). A higher-order closure model for canopy flow. *Journal of Applied Meteorology, 16*(11), 1197–1205. https://doi.org/10.1175/1520-0450(1977)016%3C1197:AHOCMF%3E2.0.CO;2

Peer-review history:
The peer review history for this paper can be accessed here:
https://pr.sdiarticle5.com/review-history/163173